Y. Lu, X. Huang*, L. Hu*, C. Fernandez-Pello (2019) *Concurrent flame spread over the horizontal thin electrical wires*, Fire Technology, 55, 193–209. https://doi.org/10.1007/s10694-018-0785-0

This is the Pre-Published Version.

Concurrent flame spread and blow-off over horizontal thin electrical wires

Yong Lu[a], Xinyan Huang[b,*], Longhua Hu[a,*], Carlos Fernandez-Pello[c]

[a]*State Key Laboratory of Fire Science, University of Science and Technology of China, Hefei, Anhui, China*

[b]*Department of Building Service Engineering, The Hong Kong Polytechnic University, Kowloon, Hong Kong*

[c]*Department of Mechanical Engineering, University of California, Berkeley, CA, USA*

***Corresponding Authors:** Xinyan Huang xy.huang@polyu.edu.hk and Longhua Hu hlh@ustc.edu.cn

Abstract: Electrical wires with the flammable polymer insulation and the metal core are responsible for many fire accidents in buildings, nuclear power plants, aircraft, and spacecraft. For the first time, this work studies the horizontal flame spread and blow off under the concurrent airflows over the thin copper-core wires. Four wires of about 1-mm diameter with different insulation thicknesses and core diameters are tested in a horizontal wind tunnel. Results show that as the concurrent airflow velocity increases, the flame spread rate first quickly increases to a maximum value, and then slightly decreases until blow-off at about 2 m/s. Heat transfer analysis shows that the preheating from flame and core have different dependences on the airflow. The flame spread is slower for a larger copper core diameter because the heat-sink effect of the core is highlighted by increasing the thermal inertia. We found a critical Froude number of 3.6 which helps determine the critical concurrent airflow velocity when the fastest flame spread is achieved. This study not only provides valuable information about the worst scenario of wire fires but also advances the fundamental understanding of the concurrent flame spread mechanism over thin fuels.

***Keywords**: Horizontal concurrent flow; Electrical wire; copper core; Froude number.*

Nomenclature

Symbols

c	specific heat (kJ/kg/K)
d	diameter (mm)
Da	Damkohler number (-)
E	activation energy (kJ/mol)
Fr	Froude number (-)
g	garvity acceleration (m/s^2)
Gr	Grashof number (-)
h	convection coefficient (W/m^2-K)
H_0	flame height without airflow (m)
k	slope (-)
L	heating length (m)
Nu	Nusselt number (-)
$\dot{q}''$	heat flux (kW/m^2)
R	universal gas constant (J/mol-K)
Re	Reynolds number (-)
V_f	flame-spread rate (mm/s)
t	time (s)
T	temperature (°C)
U	airflow velocity (m/s)
Z	pre-exponential factor (s^{-1})

Greeks

α	Thermal diffusivity (m^2/s)
δ	thickness (mm)
ρ	density (kg/m^3)
λ	thermal conductivity (W/m-K)

superscripts

*	critical

subscripts

∞	ambient
b	burning
c	core
ex	extinction
f	flame
F	fuel
g	gas
o	outer
O	oxygen
p	plastic insulation
py	pyrolysis

1. Introduction

Ignition and flame spread over electrical wire used in the electric devices is the most likely cause of fire accident in buildings [1,2], nuclear power plants [3,4], aircraft [5], and spacecraft [6]. Thus, there is a need for understanding the flame spread behaviours over the electrical wire and its extinction in various environmental conditions. The mechanism of flame spread over electrical wires is complicated, because there is a metal core inside the wire and phase-change process during combustion. Bekham *et al.* [7,8] first used the laboratory wires, which were made by coating polyethene (PE) on the copper (Cu) rods of about 1 mm thick, to study the flame spread and extinction behaviours in the wire. Fujita and co-workers carried out more extensive works on flame spread behaviours over similar thin laboratory wires under low-velocity opposed airflow and investigated the ignition [9], flame spread [10], extinction limit [11] under normal-gravity and microgravity conditions. Nakamura *et al.* [12] found that the opposed flame spread in the thin wire can be driven by either the heating from the core or flame, depending on the thermal conductivity of the metallic core. Thus, the core acted as a heat source, different from as a heat sink during the ignition process by external heating [13,14]. On the other hand, near the extinction limit, the core was found to be a heat sink [11,15,16]. To the authors' best knowledge, so far there is no study on the flame spread behaviours over electrical wires under concurrent airflow, although this scenario is common in many real wire fire accidents.

Compared to extensive researches on the opposed flame spread, only limited works have been studied the concurrent flame spread. One reason is that under a concurrent airflow the flame spread tends to accelerate and does not reach a steady state in the small-scale experiment. Nevertheless, a better understanding of the concurrent flame spread is important because it often represents one of the worst fire scenarios. Markstein and de Ris [17] showed that the flame spread over thin textile eventually reached the steady state under the concurrent buoyancy flow. Loh and Fernandez-Pello [18,19] found that the concurrent flame spread rates over both horizontally placed thin paper and thick PMMA sheets increased linearly with the concurrent airflow velocity. However, when the concurrent air flow velocity exceeded about 1 m/s, the flame spread over thin paper became insensitive to flow until blow-off. Olson and Miller [20] showed that in microgravity the rate of flame spread over the small-scale thin paper in concurrent flow also increased linearly with the low free-stream velocity. Nagachi *et al.* [21,22] investigated the concurrent flame spread over thin wires in microgravity. Larger-scale microgravity experiment of concurrent flame spread over thin fabric has also been recently conducted in the Cygnus spacecraft [23].

In this work, thin laboratory wires of about 1-mm thick with a copper core of different diameters are tested in a horizontal wind tunnel. The concurrent flame spread dynamics under different wind speeds are analysed based on experimental observation. The extinction limit and the role of the core are discussed with a heat transfer analysis.

2. Experiment

Laboratory experiments were carried out in a wind tunnel, as illustrated in Fig. 1. This wind tunnel has a cross-section of 1.5 m wide and 1.3 m high, with a total length of 72 m to ensure the flow to be fully developed and uniform [24,25]. A self-designed experimental device for studying wire fire was positioned inside the wind tunnel along the tunnel axis line, i.e., parallel to airflow. The upstream airflow velocity was monitored by a three-probe hot-wire anemometer that was placed at 0.5 m ahead of the setup. The maximum concurrent airflow velocity applied in the experiments was 2.5 m/s.

Tested thin laboratory wires have a thin outer diameter (d_o) of about 1-mm, and they are made of polyethene (PE) insulation and copper (Cu) core with different insulation thicknesses (δ_p) and core diameters (d_c). They are similar to those used in [6,10,12,26], and Table 1 and 2 lists detailed configurations of four wire and the properties of the PE insulation and Cu core. The wire sample length is 40 cm that is long enough for flame to spread beyond the effect of ignition zone and reach the steady state. The sample holders and heater coil are thin and small so that their disturbance to flow is negligible.

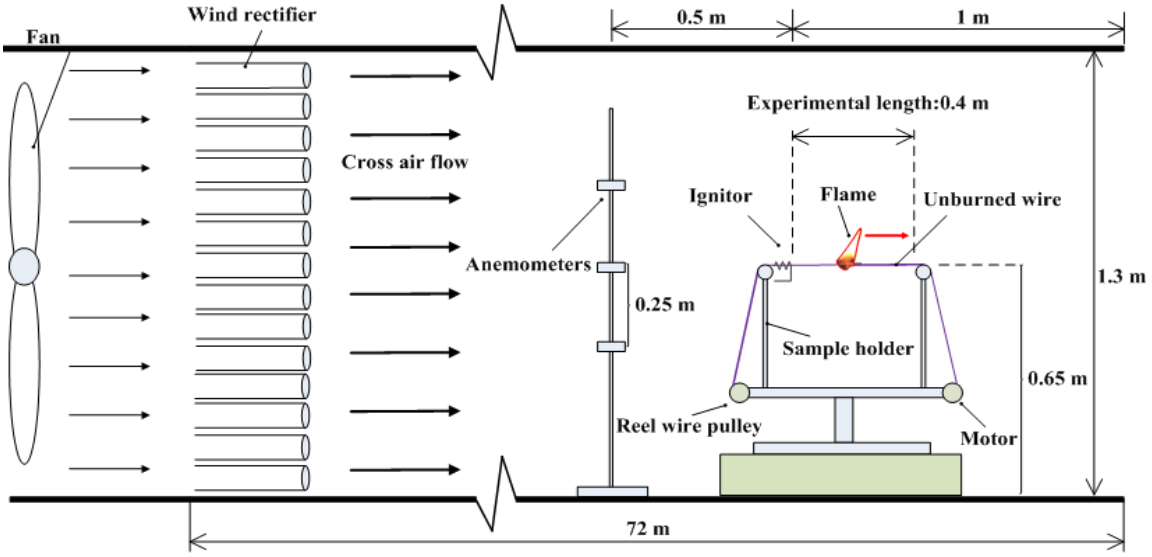

Fig. 1 Experimental setup for concurrent flame spread over a thin wire inside a wind tunnel.

Table 1. Configurations of tested electrical wire

Sample	d_o (mm)	d_c (mm)	δ_p (mm)	d_c/d_o
#1	0.60	0.30	0.15	0.50
#2	0.80	0.50	0.15	0.63
#3	1.10	0.80	0.15	0.73
#4	1.40	0.80	0.30	0.57

Table 2. Properties of PE insulation and Cu core.

	PE	Cu
Density, ρ [kg/m^3]	940	8880
Specific heat, c [kJ/kg/K]	2.15	0.39
Conductivity, λ [W/m/K]	0.30	398
Melting point, T_m [°C]	115~120	1085
Pyrolysis temperature, T_{py} [°C]	380~400	-

All the experiments were conducted at a pressure of 1 atm and an air temperature of 26 ℃. The electrical wire was ignited by a coil heater (heating for about 10 s) at the upstream end. Once the flame was stabilized, the ignition current was immediately cut-off. In each case, experiments were repeated three times. The flame-spread process was recorded by a CCD camera video (25 frames per second, resolution of 3M pixels), and the pixels were calibrated using a ruler in prior to each experiment. The background wall was covered with black masking paper to avoid reflection of any optical noise. The flame shape and spread rate were processed with an in-house MATLAB code.

3. Experimental Results

3.1. Flame spread behaviours

Figure 2(a) shows the typical photos of spreading flames with increasing concurrent (forward) airflow velocities for different sample wires. In general, as the concurrent airflow velocity increases, the flame tilts and elongates. At an airflow velocity less than 1 m/s, the flame only tilts, but its main body is still above the wire. Further increasing the airflow velocity to above 1 m/s, the whole flame envelopes the wire, which becomes almost parallel to the horizontal wire.

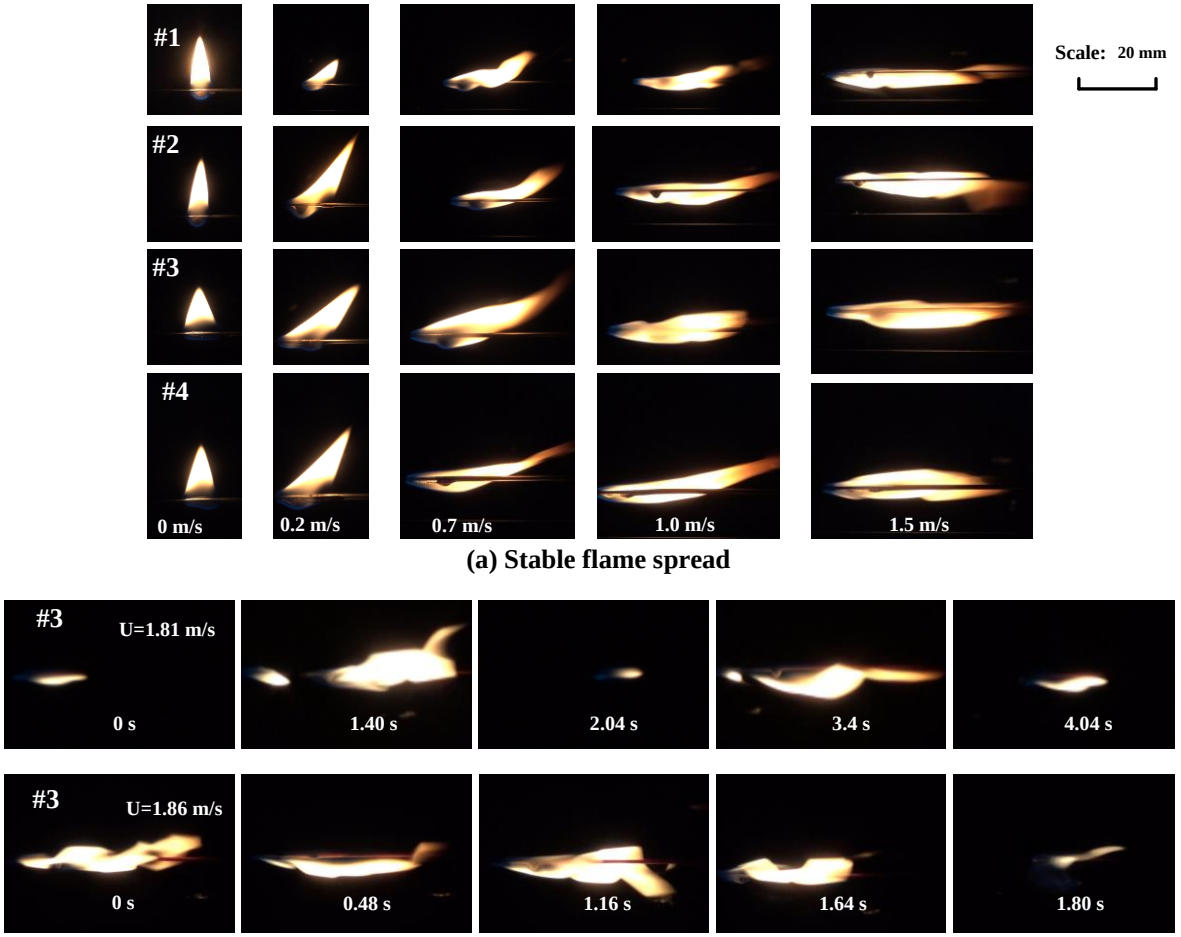

Fig. 2 Typical photos of spreading flames over the electrical wire at various concurrent airflow velocities (a) stable flame spread, and (b) extinction.

Figure 2(b) shows the blow-off phenomena when the airflow velocity is relatively high. The flame spread becomes unsteady with a periodical shrinking then expanding, like a "jump flame" over discrete fuels. The flame eventually extinguishes after several jumps. The "jump flame" is unsteady state near blow-off. At first, the small size of flame promotes the melting of PE insulation, and the molten PE start to accumulate. As the molten PE increase, the flame size becomes larger, and the upstream molten PE will be cooled and solidified due to the flow velocity. Part of the flame is blow-off while the rest is still burning, showing the behavior of "flame jump". As the flame becomes smaller, a new cycle of "flame jump" starts. Afterwards, even a slight increase in the airflow velocity can quickly blow off the flaming.

3.2. Concurrent flame spread rate

Figure 3 shows the variation of flame spread rate with an increase in the concurrent airflow velocity (U_∞) measured in the experiments and data from references. Figure 4(a) shows flame front position changing with time, and good linearity indicates that flame spread reaches the steady state, where the linear slope is flame spread rate (FSR, V_f). As the concurrent airflow velocity is increased, the FSR first increases in a nearly linear manner, and at about $U_\infty = 0.7$ m/s (the inflection point), the increase becomes faster, which trend is particularly clear for wire #2 and #3. Eventually, the FSR reaches a maximum value, and then, decreases slightly till the flame is blown-off (extinction) at about 2 m/s.

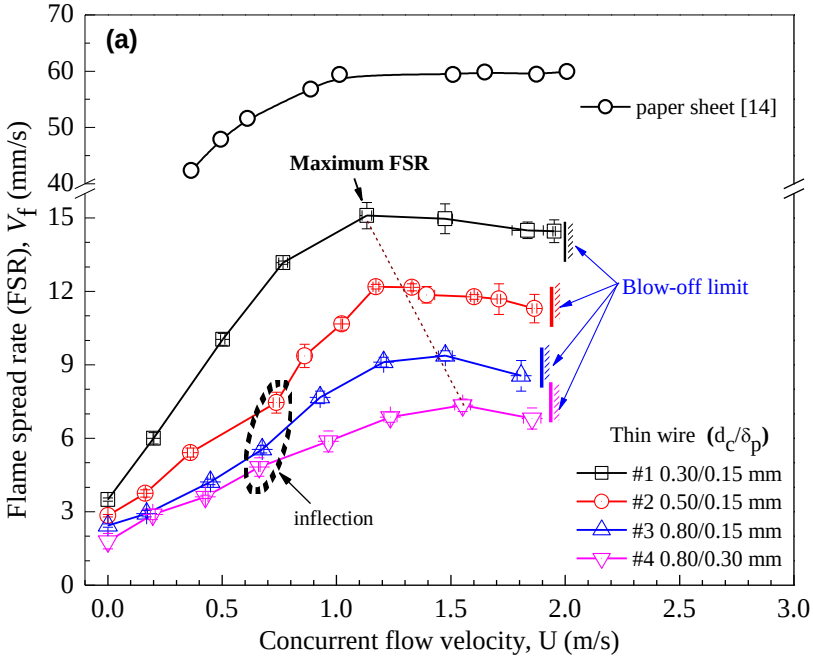

Fig. 3 Measured flame spread rate (FSR) over thin horizontal wires under the concurrent airflow.

Figure 3 also shows that there is a clear effect of wire size and configuration on the concurrent flame spread rate. As the wire diameter is decreased, the increase of FSR with airflow velocity is greater, and the measured peak FSR is larger. However, the critical concurrent airflow velocity is smaller when the maximum FSR is achieved. Also, the blow-off airflow velocity is found to be slightly larger for a smaller core diameter (comparing wire #1-3, same 0.15-mm thick insulation), and for thicker insulation (comparing wire #3 and 4, same 0.8-mm thick core).

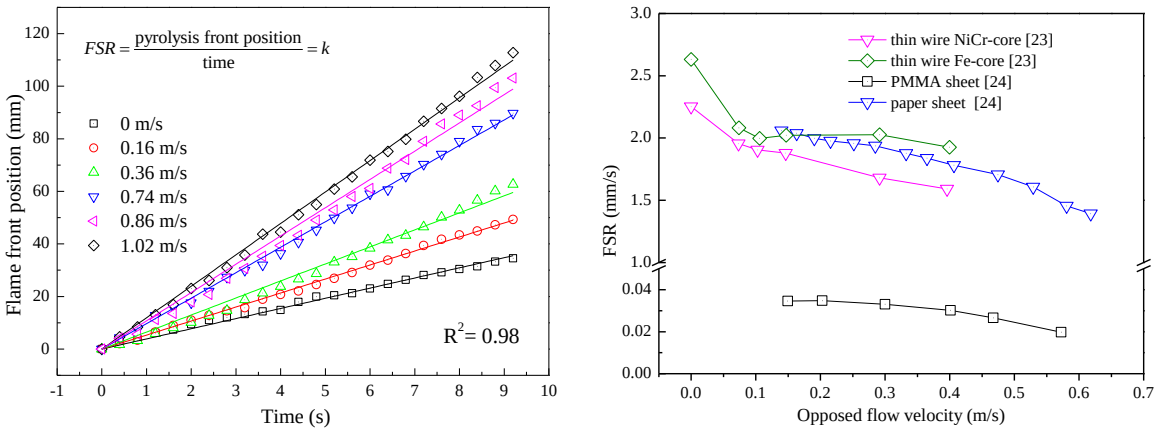

Fig. 4 (a) Flame front position over wire #2 changes with time under different concurrent flow velocities, and (b) the flame spread rate (FSR) over other thin fuels under the opposed airflow in the literature.

Comparing to the opposed flame spread of the similar thin wire [27], paper [28], and PMMA sheet [28] in Fig. 4(b), the concurrent flame spread in this work is much faster. Also, their trends in the airflow velocity are very different, as the opposed flame spread will decrease with increasing airflow. For the concurrent flame spread, its blow-off limit is much larger than that for opposed flame spread (less than 1 m/s), so it is more resistant to the wind. Moreover, compared to the concurrent flame spread over a 0.33-mm thin paper [18] in Fig. 3, the flame spread over the wire is slower because of different fuel type and geometry. However, their variation with airflow velocity is similar, i.e., both increasing to a peak value at a concurrent flow of about 1 m/s. This trend appears to be a unique feature for the thin

fuel [19]. It is also clearly different from the thick fuel [29], for which FSR increases with wind velocity [29], and no peak value can be found.

4. Discussions

4.1. Heat transfer analysis

The behaviour of flame spread over the thin wire is controlled by the heat transfer both in wire and from the flame. As illustrated in Fig. 5, there are three different regions: the preheating region, burning region, and the burn-out region. The flame spread is mainly driven by the heat transfer in the preheating region, as the measured rate of flame spread is actually the velocity of the pyrolysis front.

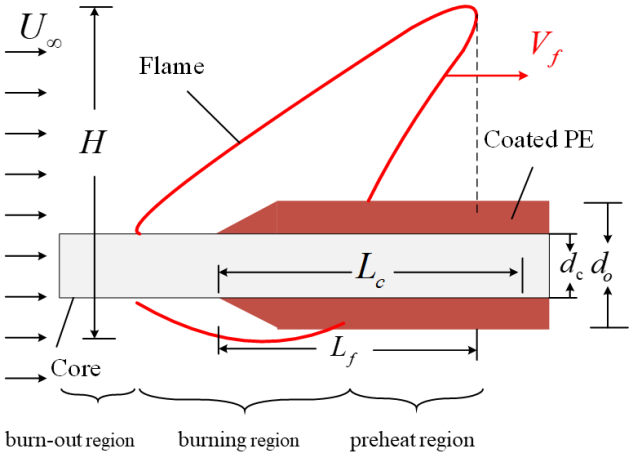

Fig. 5 Diagram of the concurrent flame spread over a thin wire.

The heat-transfer analysis for flame spread over thin fuel [30] is applied to the preheating region, and the flame spread rate could be expressed qualitatively as

$$V_f = \frac{\dot{q}_f''\left(\pi d_o L_f\right)+\dot{q}_c''\left(\pi d_c L_c\right)}{\rho_p c_p\left(T_p-T_\infty\right)\frac{\pi}{4}\left(d_o^2-d_c^2\right)+\rho_c c_c\left(T_p-T_\infty\right)\left(\frac{\pi}{4}d_c^2\right)} \sim \frac{\text{Driven Force}}{\text{Inertia}} \tag{1}$$

where $\dot{q}''$, ρ, c, and L are the heat flux, density, specific heat, and heating length, respectively, and the subscript f, p, c, and ∞ represent the flame, polymer insulation, core, and ambient, respectively. The numerator of Eq. (1), including the heating from both the flame and the wire core, represents the driving force of the flame spread. The denominator is the inertia of the flame spread ($\sum \rho cA$), which includes the change in sensible heat from ambient temperature to the pyrolysis temperature for both the solid insulation and the core.

The heat flux from the flame ($\dot{q}_f''$) includes both convection and radiation, and the convection is more sensitive to the concurrent airflow as

$$\dot{q}_{f,conv}'' = h_f\left(T_f - T_\infty\right) \tag{2a}$$

$$h_f = Nu\frac{\lambda_g}{d_o} \tag{3}$$

where λ_g is the gaseous thermal conductivity and h_f is the heat transfer coefficient of flame. Because the variation of size between wires is small, the curvature effect on convection is neglected. For the mixed natural and forced convection, the Nusselt number (Nu) can be defined by the Reynolds number

(*Re*) and the Grashof number (*Gr*) as

$$Nu = \sqrt[n]{Nu_F^n + Nu_N^n} \sim \sqrt[4]{\left(\mathrm{Re}^{1/3}\right)^4 + \left(Gr^{1/6}\right)^4} = \mathrm{Re}^{\frac{1}{3}} \sqrt[4]{1 + Fr^{-4/3}} \propto U_\infty^{\frac{1}{3}} \sqrt[4]{1 + Fr^{-4/3}} \tag{4}$$

where $n = 4$ for the cylinder [31,32], Nu_F and Nu_F are natural and forced Nusselt numbers, respectively. The Froude number (*Fr*) quantifies the relative magnitude between forced and natural convections as

$$Fr = \frac{U}{\sqrt{gH}} = \frac{\mathrm{Re}}{\sqrt{Gr}} \tag{5a}$$

where *H* is the characteristic length of buoyant flow, and it is the flame height here (Fig. 5). The value of *Fr* increases significantly with the concurrent airflow velocity (*U*), indicating a weaker buoyant effect. Moreover, the use of *Fr* number can also quantify the influence of different gravity levels on flame spread behaviours, such as in the Moon and Mars.

Based on Eqs. (3-4), the convective heat flux from the flame increases with the concurrent airflow velocity as

$$\dot{q}''_{f,conv} \sim U^{1/3} \tag{2b}$$

This correlation is particularly valid when the airflow velocity (or *Fr*) is large. In addition, the preheating length of flame (L_f) can be measured by processing the video, and the results are summarized in Fig. 6. Apparently, for all wires, the flame preheating length increases almost linearly with the concurrent airflow velocity, $L_f \sim U$, before the rate of flame spread reaches its maximum value. As seen from Eq. (1), the contribution from the flame preheating to flame spread will increase with the airflow velocity as

$$\dot{q}''_{f,conv} L_f \sim U^{4/3} \tag{6a},$$

which is slightly faster than a linear increase (see Fig. 7).

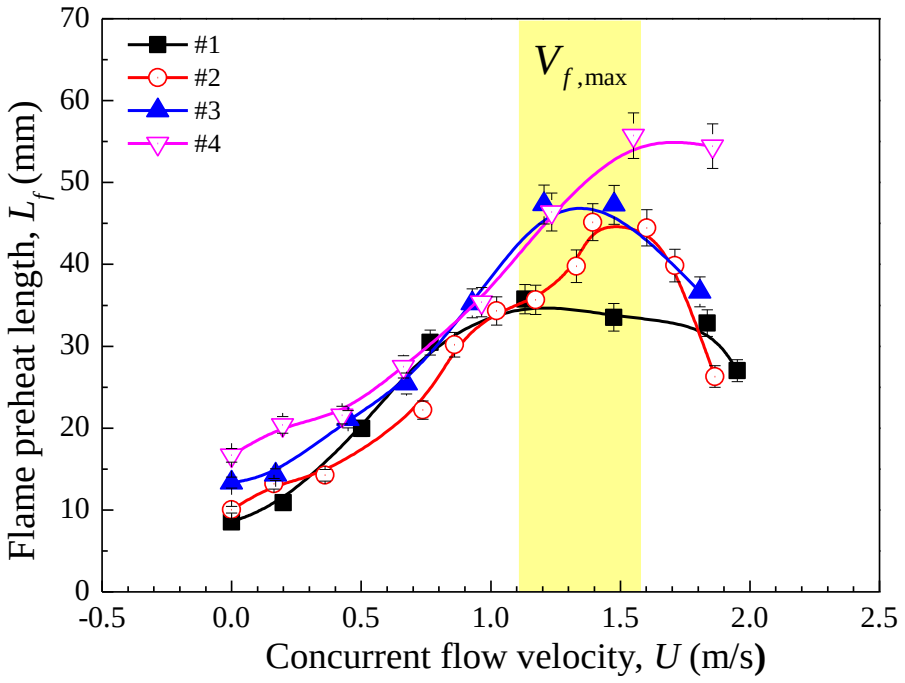

Fig. 6 Measure flame preheating length (L_f) against concurrent air flow velocity.

On the other hand, the preheating from Cu core also changes with the airflow velocity. As seen from Fig. 5, the core is heated by the flame in both the burning and burnout regions, so that its preheating heat flux should be closely related to the flame heat flux, as $\dot{q}_c'' \sim \dot{q}_f'' \sim U^{1/3}$. However, the preheating length of the core will stretch as the flame spread rate is increased, as $L_c \sim \alpha / V_f \sim U^{-1}$. Therefore, the overall contribution from the core preheating to flame spread will decrease with airflow velocity as

$$\dot{q}_c'' L_c \sim U^{-2/3} \tag{6b}$$

which becomes relatively less important in a higher airflow velocity (Fig. 7).

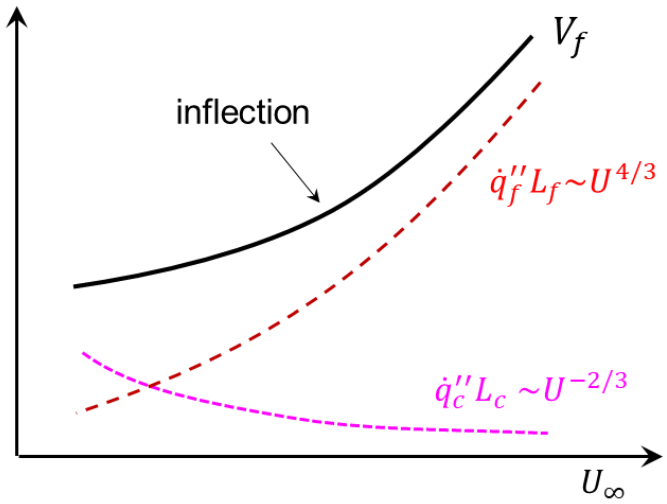

Fig. 7 The heating from the flame and core in the preheating region and FSR as a function of concurrent airflow before reaching the maximum FSR.

The actual flame spread rate is determined by the preheating from both the flame and core, as illustrated in Fig. 7. As the concurrent airflow velocity is increased, the flame spread rate increases, because the preheating from the flame is in general dominant. If the size of the core is large, the preheating from the core is also important. Then, there will be compensation between the flame and core preheating at the relatively small airflow velocity, which may lead to an inflection point in Fig. (7). This inflection point is also observed in Fig. 3 near U = 0.7 m/s for wires #2 and #3 which have a relatively larger core size.

4.2. The role of core

As seen from Eq. (1), the influence of core appears in both the numerator and the denominator, so that mathematically it acts as the "heat sink" and "heat source" at the same time. Depending on its overall effect and what it compares with, either the effect of "heat sink" or "heat source" could be highlighted.

As the concurrent wind velocity increases, eventually the preheating from the core becomes negligible (see Fig. 7). Therefore, we can conclude that in the concurrent flame spread, when the diameter of core changes, the "heat-sink" effect of the core will be highlighted by increasing the thermal inertia (ρcA). This conclusion is supported by Fig. 3 where the rate of concurrent flame spread is larger if the size of the core is smaller. Further increasing the diameter of the core, the large heat loss from the core can eventually quench the flame, especially when the flame is weak. Thus, the maximum diameter of the core or a minimum insulation thickness for flame spread could be determined [8,15].

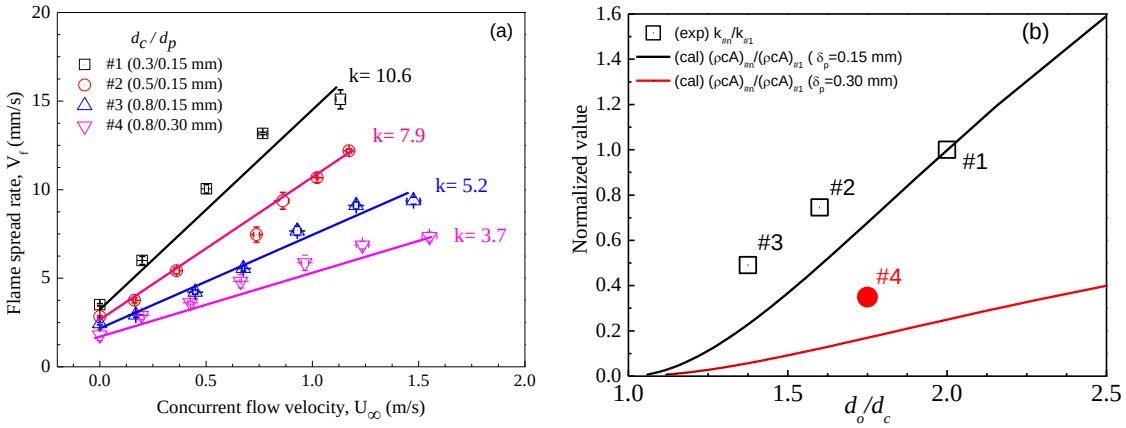

Fig. 8 (a) Linear fit between FSR and flow velocity before max FSR, and (b) comparison between the normalized slope $k_{\#n}/k_{\#1}$ and the inverse of normalized thermal inertia $\left[\left(\sum \rho cA\right)_{\#n}/\left(\sum \rho cA\right)_{\#1}\right]^{-1}$.

To describe this heat-sink effect better, Fig. 8(a) provides a linear fit for the region of fast increasing FSR in Fig. 3 before it reaches the maximum FSR, and their slope ($k_{\#n}$) is obtained. According to Eq. (1), if neglecting the preheating from the core in the numerator, the normalized slope of wire #*n* should be inversely proportional to the normalized the thermal inertia as

$$\frac{k_{\#n}}{k_{\#1}} \propto \left[\frac{\left(\sum \rho cA\right)_{\#n}}{\left(\sum \rho cA\right)_{\#1}}\right]^{-1} \tag{7}$$

Then, Fig. 8(b) shows the relative magnitude of these slopes by normalizing to the slope of wire #1 (i.e., $k_{\#n}/k_{\#1}$). For comparison, the reference curves for $\left[\left(\sum \rho cA\right)_{\#n}/\left(\sum \rho cA\right)_{\#1}\right]^{-1}$ is also plotted under varying the core diameter and insulation thickness, and the correlation in Fig. (7) captures the trend of variations between different wires. Because wire #1 has the least preheating from the core ($\dot{q}_c'' L_c$), when other wires are normalized to #1, the preheating capacity from their core will be underestimated. In other words, the gap between the point and curve in Fig. 8(b) indicates the core's minor role as the heat source. This comparison further illustrates the core's dual effect of the heat sink and heat source and supports that Eq. (1) can provide a reasonable description for the concurrent flame spread behaviour over thin wires.

On the other hand, for most heavy metals, the production of density and specific heat (ρc) almost does not change. In other words, when the core material changes from Cu to nichrome (NiCr) or iron (Fe), there will be very little change in the denominator of Eq. (1). Therefore, when the material of core changes while fixing the core size, the "heat-source" effect of the core will be highlighted by increasing the preheating from core ($\dot{q}_c'' L_c$). Such "heat-source" effect of the core has been observed in the upward (concurrent) flame spread [8], and the opposed flame spread [8,12,33] (also see Fig. 4(b)).

4.3. Maximum flame spread rate

As seen from the experiment (Fig. 2), the maximum flame spread rate is reached when the flame is pushed by the airflow to be nearly parallel to the wire. In other words, it reaches the maximum possible flame tilt angle ($\theta = 90^o$), so that geometrically the concurrent airflow can no longer enhance the flame heating. On the other hand, as the airflow velocity is further increased, the flame will be cooled by the air. Therefore, the flame spread enters from the thermal region to the chemical region, and the flame spread rate slightly decreases with the airflow velocity, as seen in Fig. 3.

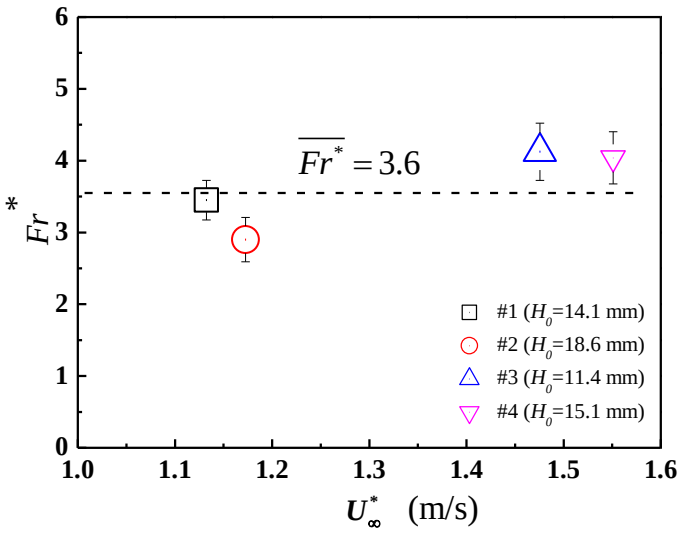

Fig. 9 Critical Froude number (Fr^*) vs. the critical concurrent airflow velocity (U^*) for the maximum flame spread rate.

The critical concurrent airflow velocity (U^*) for the maximum flame spread rate may be quantified by a critical Froude number (Fr^*) as

$$Fr^* = \frac{U^*}{\sqrt{gH_0}} \tag{5b}$$

where H_0 is the flame height without the external airflow, which can be measured from the experiment. Figure 9 shows the critical Froude number correlated to the critical airflow velocity, where the values for these four wires varies from 2.9 to 4.1, which an average value of 3.6. This critical Froude number may also be used to predict the critical airflow velocity for fastest flame spread over other wires.

4.4. Blow-off limit

Based on the above observations and discussions, the flame blow-off could be explained by a critical Damköhler number [11]

$$Da^* = \frac{t_{flow}}{t_{chem}} = \left(\frac{\alpha_g}{U_{ex}^2}\right) Y_F Y_O Z \exp\left(-\frac{E}{RT_f}\right) \tag{8}$$

where α_g is the gas diffusivity; Y_F and Y_O are the mass fraction of fuel and oxygen, respectively; R is the universal gas constant; T_f is the flame temperature; Z and E are the pre-exponential factor and activation energy of 1-step global flame chemistry, respectively.

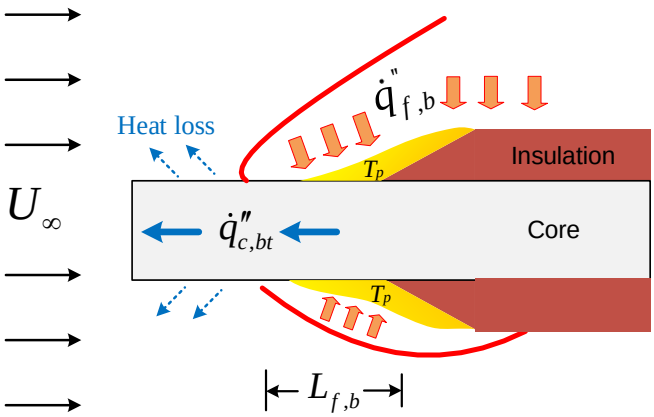

Fig. 10 Diagram of the flame over a thin wire near extinction.

Near the blow-off limit, the timescale of airflow becomes comparable with that of flame chemistry. This is evident for each tested wire that the sudden flame extinction occurs when the Da number is beyond a critical value. However, there is still a non-negligible difference in the blow-off airflow velocity (U_{ex}) for different wires (see Fig. 3), which cannot be simply explained by the critical *Da* number which only includes the gas-phase processes.

Note that as observed in Fig. 2(b) before a quick blow-off, there is an unstable jump flame which also leads to extinction in a slightly smaller airflow velocity. Therefore, there may be another criterion, related to the solid phase, co-controlling the extinction. Considering a control volume at the interface between burning and burnout region, near extinction (Fig. 10), there is a thin layer of molten insulation which is right above its pyrolysis temperature (T_{py}), and the core transfers the heat towards the cool upstream. A necessary condition to sustain a flame is to achieve a heat balance between flame heating and the cooling from the core, which is similar to a critical heating flux in the forced ignition process [13] as

$$\dot{q}_f'' L_{f,b} = \pi d_c \left(T_{py} - T_\infty\right)\sqrt{h_\infty \lambda_c d_c} \quad \Rightarrow \quad U_{ex} \propto d_c^{-6/5} \tag{9}$$

where $\dot{q}_f'' \sim U_{ex}^{1/3}$ is the flame heat flux (see Eqs. (2-4)), $L_{f,b} \approx \alpha / U_{ex}$ is the flame heating length, and $h_\infty = Nu\,\lambda_g / d_c \sim U_{ex}^{1/3}$ is the upstream convective cooling coefficient (see Eqs. (2-3)). Therefore, the blow-off airflow velocity increases with the decreasing core diameter because of the cooling effect of the core, agreeing with Fig. 3. Here, it further confirms that the core acts as a considerable "*heat sink*" role near the blow-off extinction limit, and it can change the blow-off airflow velocity a bit, even although gas-phase processes are dominant.

5. Conclusions

In this work, experimental results show that as the concurrent airflow velocity increases, the rate of flame spread over thin wire first quickly increases to a maximum value, and then slightly decreases until blow-off at about 2 m/s. Heat transfer analysis shows that for a larger copper core diameter, the rate of concurrent flame spread is slower because the larger thermal inertia of core makes it a heat sink. This is different from the heat-source effect of core found in the opposed flame spread.

We also found a critical Froude number of 3.6 to determine the critical concurrent airflow velocity when the fastest flame spread is achieved. The introduction of Froude number permits the extension of these results to different gravity levels, such as the fire phenomenon on the Moon, Mars and beyond. Also, the blow-off airflow velocity is found to be slightly smaller for a larger copper core diameter, probably because of the additional cooling from the core.

Acknowledgements

This work was supported jointly by the Key project of NSFC (No. 51636008), Newton Advanced Fellowship (No. NA140102), Key Research Program of Frontier CAS (No. QYZDB-SSW-JSC029) and Fok Ying Tong Education Foundation (No. 151056). YL also thanks for the support from CSC.

References

[1] M. Ahrens, Home Structure Fires, 2016. www.nfpa.org.

[2] B. V. Ettling, Electrical wiring in building fires, Fire Technology. 14 (1978) 317–325. doi:10.1007/BF01998391.

[3] USNRC, Cable Response to Live Fire (CAROLFIRE) Volume 1: Test Descriptions and Analysis of Circuit Response Data, 2008. http://www.nrc.gov/docs/ML0811/ML081190230.pdf.

[4] R.H. V Gallucci, Statistical Characterization of Cable Electrical Failure Temperatures Due to Fire for Nuclear Power Plant Risk Applications, Fire Technology. 53 (2017) 401–412. doi:10.1007/s10694-016-0616-0.

[5] R. Friedman, Fire Safety in Spacecraft, Fire and Materials. 20 (1996) 235–243. doi:10.1002/(SICI)1099-1018(199609)20:5<235::AID-FAM580>3.0.CO;2-Y.

[6] M. Kikuchi, O. Fujita, K. Ito, A. Sato, T. Sakuraya, Experimental study on flame spread over wire insulation in microgravity, Symposium (International) on Combustion. 27 (1998) 2507–2514. doi:10.1016/S0082-0784(98)80102-1.

[7] N. Bakhman, L. Aldabaev, B. Kondrikov, V. Filippov, Burning of polymeric coatings on copper wires and glass threads: I. Flame propagation velocity, Combustion and Flame. 41 (1981) 17–34. doi:10.1016/0010-2180(81)90036-5.

[8] N. Bakhman, L. Aldabaev, B. Kondrikov, V. Filippov, Burning of polymeric coatings on copper wires and glass threads: II. Critical conditions of burning, Combustion and Flame. 41 (1981) 35–43. doi:10.1016/0010-2180(81)90037-7.

[9] O. Fujita, T. Kyono, Y. Kido, H. Ito, Y. Nakamura, Ignition of electrical wire insulation with short-term excess electric current in microgravity, Proceedings of the Combustion Institute. 33 (2011) 2617–2623. doi:10.1016/j.proci.2010.06.123.

[10] O. Fujita, K. Nishizawa, K. Ito, Effect of low external flow on flame spread over polyethylene-insulated wire in microgravity, Proceedings of the Combustion Institute. 29 (2002) 2545–2552. doi:10.1016/S1540-7489(02)80310-8.

[11] S. Takahashi, H. Ito, Y. Nakamura, O. Fujita, Extinction limits of spreading flames over wires in microgravity, Combustion and Flame. 160 (2013) 1900–1902. doi:10.1016/j.combustflame.2013.03.029.

[12] Y. Nakamura, N. Yoshimura, H. Ito, K. Azumaya, O. Fujita, Flame spread over electric wire in sub-atmospheric pressure, Proceedings of the Combustion Institute. 32 (2009) 2559–2566. doi:DOI 10.1016/j.proci.2008.06.146.

[13] X. Huang, Y. Nakamura, F.A.A. Williams, Ignition-to-spread transition of externally heated electrical wire, Proceedings of the Combustion Institute. 34 (2013) 2505–2512. doi:10.1016/j.proci.2012.06.047.

[14] X. Wang, H. He, L. Zhao, J. Fang, J. Wang, Y. Zhang, Ignition and Flame Propagation of Externally Heated Electrical Wires with Electric Currents, Fire Technology. 52 (2016) 533–546. doi:10.1007/s10694-015-0515-9.

[15] K. Miyamoto, X. Huang, N. Hashimoto, O. Fujita, C. Fernandez-Pello, Limiting Oxygen Concentration (LOC) of Burning Polyethylene Insulated Wires under External Radiation, Fire Safety Journal. 86 (2016) 0–17. doi:10.1016/j.firesaf.2016.09.004.

[16] Y. Lu, X. Huang, L. Hu, C. Fernandez-Pello, The interaction between fuel inclination and forward wind: Experimental study using thin wire, Proceedings of the Combustion Institute. 000 (2018) 1–8. doi:10.1016/j.proci.2018.05.131.

[17] G.H. Markstein, J. De Ris, Upward fire spread over textiles, Symposium (International) on Combustion. 14 (1973) 1085–1097.

[18] H.T. Loh, A.C. Fernandez-Pello, A study of the controlling mechanisms of flow assisted flame spread, Symposium (International) on Combustion. 20 (1985) 1575–1582. doi:http://dx.doi.org/10.1016/S0082-0784(85)80652-4.

[19] H.T. Loh, C.A. Fernandez-pello, Flow Assisted Flame Spread over Thermally Thin Fuels, Fire Safety Science. 1 (1986) 65–74. http://www.iafss.org/publications/fss/1/65.

[20] S.L. Olson, F.J. Miller, Experimental comparison of opposed and concurrent flame spread in a forced convective microgravity environment, Proceedings of the Combustion Institute. 32 (2009) 2445–2452. doi:10.1016/j.proci.2008.05.081.

[21] M. Nagachi, F. Mitsui, J. Citerne, H. Dutilleul, A. Guibaud, G. Jomaas, G. Legros, N. Hashimoto, O. Fujita, Effect of Flow Direction on the Extinction Limit for Flame Spread over Wire Insulation in Microgravity, in: 47th International Conference on Environmental Systems, 2017: p. 244.

[22] M. Nagachi, F. Mitsui, J.-M. Citerne, H. Dutilleul, A. Guibaud, G. Jomaas, G. Legros, N.

Hashimoto, O. Fujita, Can a spreading flame over electric wire insulation in concurrent flow achieve steady propagation in microgravity?, Proceedings of the Combustion Institute [in Press]. 37 (2018). doi:10.1016/j.proci.2018.05.007.

[23] G. Jomaas, J.L. Torero, C. Eigenbrod, J. Niehaus, S.L. Olson, P. V Ferkul, G. Legros, A.C. Fernandez-Pello, A.J. Cowlard, S. Rouvreau, N. Smirnov, O. Fujita, J.S. T 'ien, G.A. Ruff, D.L. Urban, Fire safety in space – beyond flammability testing of small samples, Acta Astronautica. 109 (2015) 208–216. doi:10.1016/j.actaastro.2014.11.025.

[24] L. Hu, S. Liu, J.L. de Ris, L. Wu, A new mathematical quantification of wind-blown flame tilt angle of hydrocarbon pool fires with a new global correlation model, Fuel. 106 (2013) 730–736. doi:10.1016/j.fuel.2012.10.075.

[25] L. Hu, J. Hu, S. Liu, W. Tang, X. Zhang, ScienceDirect Evolution of heat feedback in medium pool fires with cross air flow and scaling of mass burning flux by a stagnant layer theory solution, PROCEEDINGS OF THE COMBUSTION INSTITUTE. 35 (2014) 2511–2518. doi:10.1016/j.proci.2014.06.074.

[26] O. Fujita, M. Kikuchi, K. Ito, K. Nishizawa, Effective mechanisms to determine flame spread rate over ethylene-tetrafluoroethylene wire insulation: Discussion on dilution gas effect based on temperature measurements, Proceedings of the Combustion Institute. 28 (2000) 2905–2911. doi:10.1016/S0082-0784(00)80715-8.

[27] Y. Nakamura, N. Yoshimura, T. Matsumura, H. Ito, O. Fujita, Opposed-wind Effect on Flame Spread of Electric Wire in Sub-atmospheric Pressure, Journal of Thermal Science and Technology. 3 (2008) 430–441. doi:10.1299/jtst.3.430.

[28] A.C. Fernandez-Pello, S.R. Ray, I. Glassman, Flame spread in an opposed forced flow: the effect of ambient oxygen concentration, Symposium (International) on Combustion. 18 (1981) 579–589. doi:10.1016/S0082-0784(81)80063-X.

[29] H. Loh, A study of the controlling mechanisms of flow assisted flame spread, Twentieth Symposium (International) on Combustion. 117 (1984) 1575–1582.

[30] J.G. Quintiere, Fundamentals of fire phenomena, John Wiley, 2006.

[31] T.L. Bergman, A.S. Lavine, F.P. Incropera, D.P. DeWitt, Fundamentals of heat and mass transfer, 2011, USA: John Wiley & Sons ISBN. 13 (2015) 470–978.

[32] C.-P. Mao, A.C. Fernandez-Pello, P.J. Pagni, Mixed convective buring of a fuel surface with arbitrary inclination, J Heat Transfer. 106 (1984) 304–309. doi:10.1115/1.3246673.

[33] Y. Kobayashi, X. Huang, S. Nakaya, M. Tsue, C. Fernandez-Pello, Flame spread over horizontal and vertical wires: The role of dripping and core, Fire Safety Journal. 91 (2017) 112–122. doi:10.1016/j.firesaf.2017.03.047.